Three body unitary coupled channel analysis on $\eta(1405/1475)$

Jia-Jun Wu[1,2,*], *Satoshi X.* Nakamura[3,4,5,**], *Qi* Huang[6,***], *Hai-Ping* Peng[4,5,****], *Yan* Zhang[4,5,†], and *Ying-Chun* Zhu[4,5,‡]

[1]School of Physical Sciences, University of Chinese Academy of Sciences (UCAS), Beijing 100049, China
[2]Southern Center for Nuclear-Science Theory (SCNT), Institute of Modern Physics, Chinese Academy of Sciences, Huizhou 516000, Guangdong Province, China
[3]Institute of Frontier and Interdisciplinary Science, Shandong University, Qingdao 266237, China
[4]University of Science and Technology of China, Hefei 230026, China
[5]State Key Laboratory of Particle Detection and Electronics (IHEP-USTC), Hefei 230036, China
[6]Department of Physics, Nanjing Normal University, Nanjing, Jiangsu 210097, China

Abstract. The new BESIII data on $J/\psi \to \gamma\eta(1405/1475) \to \gamma K\bar{K}\pi$ is more precise than before. A three-body unitary coupled-channel analysis of experimental Monte Carlo outputs for $J/\psi \to \gamma\eta(1405/1475) \to \gamma K\bar{K}\pi$ is introduced. This model does not only fit the $K\bar{K}\pi$ Dalitz plot distributions but also the branching ratios of "$\gamma\pi\pi\eta$" and "$\gamma\gamma\pi\pi$" final states relative to that of "$\gamma K\bar{K}\pi$". After fitting, we successfully extract the $\eta(1405/1475)$ pole locations. The $\eta(1405/1475)$ states are described by two bare states dressed with continuum states. At last, we post predict the distribution of $J/\psi \to \gamma\eta(1405/1475) \to \gamma\pi\pi\eta, \gamma\pi\pi\pi, \gamma\gamma\pi\pi$.

1 Introduction

In 1967 [1], from the annihilation $p\bar{p} \to K\bar{K}\pi\pi\pi$, the authors first observed an enhancement in the $K\bar{K}\pi$ neutral system around the region 1.4 – 1.5 GeV. By using Briet-Wigner (BW) amplitudes, the authors extracted a light isoscalar pseudoscalar state, later named as $\eta(1405/1475)$. Until now, there still remain two main puzzling issues: (i) Is $\eta(1405/1475)$ one or two η excited states in this energy region? (ii) What is the internal structure of the excited state(s)? For the first puzzle, $\eta(1405/1475)$ has been observed in various processes while the spectrum peak locations are different. Roughly speaking, there is only one peak in $\eta\pi\pi$ final states [2–6], while there are structures due to two overlapping peaks in the $K\bar{K}\pi$ final state [7–11]. In the conventional quark model, meanwhile, there are only two radially excited η and η' states here, corresponding to $\eta(1295)$ and $\eta(1405/1475)$. However, if $\eta(1405/1475)$ include two η^* states, what is the extra η state here? Actually, $\eta(1405/1475)$

* e-mail: wujiajun@ucas.ac.cn
** e-mail: satoshi@sdu.edu.cn
*** e-mail: huangqi@ucas.ac.cn
**** e-mail: penghp@ustc.edu.cn
† e-mail: zhy02424@mail.ustc.edu.cn
‡ e-mail: yingchun@ustc.edu.cn

states are coupled with various hadronic channels, two-body and three-body systems, and a glueball is another interpretation here. The conventional quark model does not account for these effects.

On the experimental side, it is common practice to use Breit-Wigner amplitudes in the attempt to extract masses, widths and the number of contributing states. In fact, when a resonance is close to the threshold of its decay channel or two resonances are overlapping, the BW amplitude is unsuitable since the unitary is not respected [12]. Here, $\eta(1405/1475)$ is very close to the $K^*\bar{K}$ threshold, and the two possible η^* resonances overlap strongly. Thus, the analysis needs a full unitary model to understand the bump of $\eta(1405/1475)$.

Recently, based on 126436 events of $J/\psi \to \gamma K_S K_s \pi^0$, BESIII collaboration perform a partial wave analysis [13], including $J^{PC} = 0^{-+}$, 1^{++}, and 2^{++}. They used a bin-by-bin analysis for the $K_S K_s \pi^0$ final state to extract the contribution of $J^{PC} = 0^{-+}$, i.e., $\eta(1405/1475)$. When they build the amplitude of $J/\psi \to \gamma\eta(1405/1475) \to \gamma K_S K_S \pi^0$, they first determined various two-body contributions such as $K^*\bar{K}$ and $a_0(980)\pi$ at each of $K_S K_S \pi^0$ energies. Such two-body contributions are described by the BW form which is not appreciated here. However, since the efficiency correction is almost model independent and pseudo data combining with the efficiency correction has described the data very well, such pseudo data can be used for further investigation. We will introduce new results based on a three-body unitary coupled-channel model. The model is fitted to the $K_S K_S \pi^0$ Dalitz plot pseudo-data generated from BESIII's 0^{-+} amplitude. Furthermore, the branching fractions of other final states such as $\eta\pi^+\pi^-$ and $\rho^0\gamma$ relative to that of $K\bar{K}\pi$ are fitted to constrain the model.

2 Three-body unitary coupled-channel model

In this section, we will broadly introduce the formalism in that can be found in more detail in Ref. [15]. The partial decay width of radiative decay $J/\psi \to \gamma\eta(1405/1475) \to \gamma(abc)$ can be written as,

$$\frac{d\Gamma_{J/\psi\to\gamma\eta(1405/1475)\to\gamma(abc)}}{dE} = \frac{2E^2}{\pi}\sum_{ij}\sum_{k\ell} d\Gamma^{ik}_{\eta^*\to abc}\frac{[\bar{G}_{\eta^*}(E)]_{ij}}{\sqrt{m_{\eta^*_i}m_{\eta^*_j}}}\frac{[\bar{G}_{\eta^*}(E)]^*_{k\ell}}{\sqrt{m_{\eta^*_k}m_{\eta^*_\ell}}}\Gamma^{j\ell}_{J/\psi\to\eta^*\gamma}\,, \quad (1)$$

$$d\Gamma^{ij}_{\eta^*\to abc} \equiv \mathcal{B}\frac{\mathcal{M}_{\eta^*_i\to abc}\,\mathcal{M}^*_{\eta^*_j\to abc}}{(2\pi)^3\,32\,E^3}dm^2_{ab}\,dm^2_{ac}\,, \quad (2)$$

$$\Gamma^{ij}_{J/\psi\to\eta^*\gamma} \equiv \frac{1}{8\pi}\frac{p_\gamma}{m^2_{J/\psi}}\mathcal{M}_{J/\psi\to\eta^*_i\gamma}\mathcal{M}^*_{J/\psi\to\eta^*_j\gamma}\,. \quad (3)$$

where E is the total energy of (abc) system and m_α is the mass of particle α; $[\bar{G}_{\eta^*}(E)]$ is the propagator matrix of η^* with invariant mass E, where its indices indicate the $i-$ and $j-$ η^* states; m_{ab} and m_{ac} are the invariant masses of the ab and ac subsystems, respectively; p_γ denotes the photon momentum in the J/ψ-at-rest frame; $\mathcal{M}_{J/\psi\to\eta^*\gamma}$ and $\mathcal{M}_{\eta^*_i\to abc}$ are the invariant amplitudes of the corresponding processes. A Bose factor $\mathcal{B}$ is: $\mathcal{B} = 1/3!$ for identical three particles abc; $\mathcal{B} = 1/2!$ for identical two particles among abc; $\mathcal{B} = 1$ otherwise.

For $\mathcal{M}_{J/\psi\to\eta^*\gamma}$, we have,

$$\mathcal{M}_{J/\psi\to\eta^*_j\gamma} = g_{J/\psi\eta^*_j\gamma}\,(\vec{\epsilon}_{J/\psi}\times\vec{\epsilon}_\gamma)\cdot\vec{p}_\gamma\,, \quad (4)$$

where $\vec{\epsilon}_\alpha$ is the polarization of particle α.

For the $\mathcal{M}_{\eta^*_i\to abc}$, we have,

$$\mathcal{M}_{\eta^*_i\to abc} = -(2\pi)^3\sqrt{16m_{\eta^*_i}E_aE_bE_c}\sum_{abc}^{\text{cyclic}}\sum_{RR's^z_R}\Gamma_{ab,R}\,\tau_{R,R'}(p_c,E-E_c)\,\bar{\Gamma}_{cR',\eta^*_i}(\vec{p}_c,E), \quad (5)$$

where cyclic permutations $(abc), (cab), (bca)$ are indicated by $\sum_{abc}^{\text{cyclic}}$. The $R \to ab$ vertex $\Gamma_{ab,R}$ is given by

$$\Gamma_{ab,R} = (t_a t_a^z t_b t_b^z | t_R t_R^z) Y_{s_R, s_R^z}(\hat{\vec{p}}_a^*) \sqrt{\frac{m_R E_a(p_a^*) E_b(p_a^*)}{E_R(p_c) E_a(p_a) E_b(p_b)}} f_{ab,R}(p_a^*), \tag{6}$$

$$f_{ab,R}(q) \equiv g_{ab,R} \frac{(1 + q^2/c_{ab,R}^2)^{-2-\frac{L}{2}}}{\sqrt{m_R E_a(q) E_b(q)}} \frac{q^L}{m_\pi^{L-1}}, \tag{7}$$

where the parentheses are Clebsch-Gordan coefficients, and t_x and t_x^z are the isospin of a particle x and its z-component, respectively; $\vec{p}_a^*$ ($p_a^* = |\vec{p}_a^*|$) denotes a particle a's momentum in the ab CM frame. The coupling $g_{ab,R}$ and cutoff $c_{ab,R}$ in Eq. (7), and the bare mass m_R in Eq. (6) are determined by analyzing L-wave ab scattering data [14, 15].

The dressed R propagator $\tau_{R,R'}(p, E)$ is given by

$$[\tau^{-1}(p, E)]_{R,R'} = [E - E_R(p)]\delta_{R,R'} - \Sigma_{R,R'}(p, E), \tag{8}$$

with the R self-energy

$$\Sigma_{R,R'}(p, E) = \sum_{ab} (t_a t_a^z t_b t_b^z | t_R, t_a^z + t_b^z)(t_a t_a^z t_b t_b^z | t_{R'}, t_a^z + t_b^z) \times \sqrt{\frac{m_R m_{R'}}{E_R(p) E_{R'}(p)}} \int q^2 dq \frac{M_{ab}(q)}{\sqrt{M_{ab}^2(q) + p^2}} \frac{\mathcal{B}_{ab} f_{R,ab}(q) f_{ab,R'}(q)}{E - \sqrt{M_{ab}^2(q) + p^2} + i\epsilon}, \tag{9}$$

with $M_{ab}(q) = E_a(q) + E_b(q)$; R and R' in Eq. (9) have the same spin state ($s_R = s_{R'}$). $\mathcal{B}_{ab}$ is the Bose symmetry factor with $\mathcal{B}_{ab} = 1 - 1/2\delta_{ab}$.

The dressed $\eta_i^* \to Rc$ decay vertex $\bar{\Gamma}_{cR,\eta_i^*}(\vec{p}_c, E)$ is given by

$$\bar{\Gamma}_{cR,\eta_i^*}(\vec{p}_c, E) = (t_R t_R^z t_c t_c^z | t_{M^*} t_{M^*}^z) Y_{S_R, S_R^z}(-\hat{\vec{p}}_c) \bar{F}_{\eta_i^* cR}(p_c, E), \tag{10}$$

The dressed $\eta_i^* \to Rc$ vertex function is

$$\bar{F}_{\eta_i^* cR}(p_c, E) = F_{\eta_i^* cR}(p_c) + \sum_{c'R'R''} \int q^2 dq X_{cR,c'R''}^{J^{PC}}(p_c, q; E) \tau_{R'',R'}(q, E - E_{c'}) F_{\eta_i^* c'R'}(q), \tag{11}$$

where a bare vertex function includes a dipole form factor as

$$F_{\eta_i^* cR}(q) = C_{cR}^{\eta_i^*} \frac{[1 + q^2/(\Lambda_{cR}^{\eta_i^*})^2]^{-2-\frac{S_R}{2}}}{\sqrt{8 E_c(q) E_R(q)\, m_{\eta_i^*}}} \frac{q^{S_R}}{m_\pi^{S_R - 1}}, \tag{12}$$

where $C_{cR}^{\eta_i^*}$ and $\Lambda_{cR}^{\eta_i^*}$ are coupling and cutoff parameters, respectively. We also have introduced J^{PC} partial wave amplitudes for $cR \to c'R'$ scatterings, $X_{cR,c'R''}^{J^{PC}}(p_c, q; E)$, that is obtained by solving the scattering equation:

$$X_{c'R',cR}^{J^{PC}}(p', p; E) = V_{c'R',cR}^{J^{PC}}(p', p; E) + \sum_{\tilde{c},\tilde{R},\tilde{\tilde{R}}} \int q^2 dq\, V_{c'R',\tilde{c}\tilde{\tilde{R}}}^{J^{PC}}(p', q; E) \tau_{\tilde{\tilde{R}},\tilde{R}}(q, E) X_{\tilde{c}\tilde{R},cR}^{J^{PC}}(q, p; E), \tag{13}$$

$$V_{c'R',cR}^{J^{PC}}(p', p; E) \equiv Z_{c'R',cR}^{\bar{c},J^{PC}}(p', p; E) + v_{c'R',cR}^{HLS,J^{PC}}(p', p). \tag{14}$$

The $Z^{\bar{c},J^{PC}}_{c'R',cR}$ is called Z-diagram, where $\bar{c}$ indicates an exchanged particle. The $v^{HLS,J^{PC}}_{c'R',cR}$ is a vector-meson exchange mechanism based on the hidden local symmetry model [16].

At last, the dressed η^* propagator in Eq. (1) is given by

$$\left[\bar{G}^{-1}_{\eta^*}(E)\right]_{ij} = (E - m_{\eta^*_i})\delta_{ij} - \mathcal{B}_{Rc} \sum_{cRR'l} \int q^2 dq\, F_{cR,\eta^*_i}(q)\tau_{R,R'}(q, E - E_c(q))\bar{F}_{\eta^*_j cR'}(q, E). \quad (15)$$

In our model, since two-body parameters in Eq. (7) have been fixed, we only adjust the parameters $g_{J/\psi\eta^*_i\gamma}$, bare masses of η^* and $C^{\eta^*_i}_{cR}$ in Eq. (12) for the various couplings between η^*_i and Rc channels. Here we include $K^*\bar{K}$, $\kappa\bar{K}$, $a_0(980)\pi$, $a_2(1320)\pi$, $f_0(980)\eta$ and $f_0(980)\pi$ channels as Rc. In addition, we also consider the non-resonant amplitudes, and $\rho\rho$ channel for higher η^* state, for which details are given in Ref. [15].

3 The results of fitting

In this calculation, we fit the $K\bar{K}\pi$ Dalitz plots over $E = [1300, 1600]$ MeV. We divide the E-region into 30 bins with 10 MeV width. In each E bin, we divide Dalitz plot spanned by the $K_S K_S$ and $K_S\pi^0$ invariant mass squared into 50×50 bins. The statistical uncertainties are $\sqrt{N}$ where N is the number of events in a bin specified by the E-bin and the Dalitz plot bin. Furthermore, we also fit the model to the two ratios below,

$$R_1^{\rm exp} = \frac{\Gamma[J/\psi \to \gamma\eta(1405/1475) \to \gamma(K\bar{K}\pi)]}{\Gamma[J/\psi \to \gamma\eta(1405/1475) \to \gamma(\eta\pi^+\pi^-)]} = \frac{(2.8 \pm 0.6)\times 10^{-3}}{(3.0 \pm 0.5)\times 10^{-4}} = 6.8 - 11.9\,, \quad (16)$$

$$R_2^{\rm exp} = \frac{\Gamma[J/\psi \to \gamma\eta(1405/1475) \to \gamma(\rho^0\gamma)]}{\Gamma[J/\psi \to \gamma\eta(1405/1475) \to \gamma(K\bar{K}\pi)]} = 0.015 - 0.043\,. \quad (17)$$

Other details of fitting are given in Ref. [15].

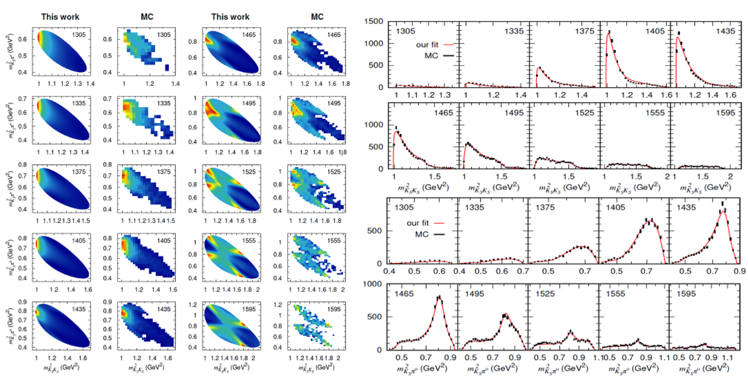

Figure 1. The Dalitz plots (left) and invariant mass spectra (right). Figures taken from Ref. [15]. Copyright(2023) APS.

The quality of fitting with two bare states is quite good as shown in Fig. 1. We also obtain the contribution of the various processes as shown in Fig. 2(left), where the main contribution is from $K^*\bar{K}$ channel. The flat structure is mainly from $K^*\bar{K}$ contribution dominated by tree diagram. The second largest contribution is mainly from triangle diagram of $\kappa\bar{K}$, which was not included in BESIII analysis. We find $a_0(980)\pi$ contribution is negligible in our model while it plays an important role in the BESIII analysis. Actually, the ratio between

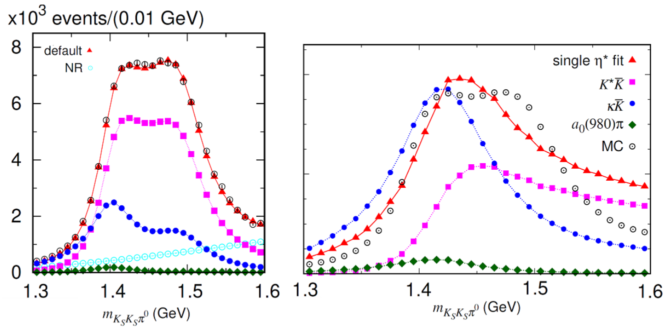

Figure 2. The $K\bar{K}\pi$ distribution with two (left) and one (right) bare state. Figures taken from Ref. [15]. Copyright(2023) APS.

$\eta^* \to \eta\pi\pi$ and $K\bar{K}\pi$ constrains the contribution from $a_0(980)\pi$, while such information was not considered in the analysis of BESIII.

In Fig. 2(right), we also show our fitting with only one bare η^* just for the $m_{K_S K_S \pi^0}(= E)$ distribution. We find that it (a red curve in Fig. 2(right)) cannot reproduce the flat peak structure. The peaks of $\kappa\bar{K}$ and $a_0\pi$ contributions are around 1420 MeV, while the peak caused by $K^*\bar{K}$ is 30 – 40 MeV higher than the mentioned two peaks because its threshold opens at $E \sim 1.4$ GeV and the $K^*\bar{K}$ pair is in a is in a relative p-wave. However, it is not sufficient to produce a flat structure with 100 MeV width. Thus, we conclude that two bare η^* states are necessary.

The bare states are mixed and dressed by meson-meson continuum states, forming the resonance states in the coupled channel model. In concept, the bare states are similar to states from a quark model or Lattice QCD without two-hadron operators. The lighter bare state around 1.6 GeV seems compatible with the excited $s\bar{s}$. The heavier one is around 2.3 GeV in our model. To be honest, those in the range of 2 – 2.4 GeV can give comparable fits. It could be either of a second radial excitation of $\eta^{(\prime)}$, a hybrid, a glueball, or a mixture of these states. We can extract the pole positions of the η^*, $(1401.6 \pm 0.6) + i(65.8 \pm 1.0)$ MeV and $(1495.0 \pm 1.5) + i(86.4 \pm 1.8)$ MeV on the unphyiscal Riemann sheet (RS) of $K^*\bar{K}$ and the physical RS of $a_2(1320)\pi$, and $1401.6 \pm 0.6 + i65.8 \pm 1.0$ MeV on the physical RS of the two channels.

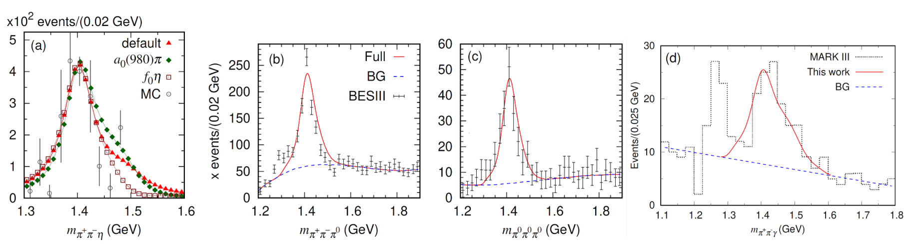

Figure 3. The post prediction of distribution of $\eta\pi^+\pi^-$(a), $\pi^+\pi^-\pi^0$(b), $\pi^0\pi^0\pi^0$(c) and $\gamma\pi^+\pi^-$(d) in the J/ψ radiative decay. Figures taken from Ref. [15]. Copyright(2023) APS.

At last, by using our model, we can post predict the distributions of $J/\psi \to \gamma\eta(1405/1475) \to \gamma\pi\pi\eta$, $\gamma\pi\pi\pi$, $\gamma\gamma\pi\pi$, as shown in Fig. 3. Typically, for the isospin breaking process of $\eta(1405/1475) \to \pi\pi\pi$, it is just generated from the loop diagram which is purely re-scattering contributions. In our model, such contributions are included automatically by respecting the three-body unitarity.

4 Summary

In this proceeding, we introduce the results of the description of $J/\psi \to \gamma\eta(1405/1475) \to \gamma K_S K_S \pi$ with a three-body unitary coupled-channel model. In this model, we systematically consider various coupled channel contributions. With two bare η^* states, we obtain a reasonable fit to the pseudo-data generated from the BESIII's Monte Carlo outputs. We also find that one bare η^* state cannot explain the current data since the flat structure can not be well described. The η^* pole positions are extracted. The η^* lineshapes extracted from the $\gamma\pi\pi\eta$, $\gamma\pi\pi\pi$ and $\gamma\gamma\pi\pi$ final states of J/ψ decay are calculated within our model, and are all well consistent with existing experimental data. In the next step, we will extend the present analysis by including more partial waves such as 1^{++} and 2^{++}, and directly analyze the BESIII data of $J/\psi \to \gamma K_S K_S \pi^0$.

5 Acknowledgments

This work is in part supported by National Natural Science Foundation of China (NSFC) under contracts U2032103, 11625523, 12175239, 12221005, 12305087, and U2032111, and also by National Key Research and Development Program of China under Contracts 2020YFA0406400, Chinese Academy of Sciences under Grant No. YSBR-101 (J.J.W.), and the Start-up Funds of Nanjing Normal University under Grant No. 184080H201B20 (Q.H.).

References

[1] P. H. Baillon *et al.* Nuovo Cim. A **50** (1967), 393-421
[2] C. Amsler et al., in $p\bar{p}$ annihilation at rest, Eur. Phys. J. C **33**, 23 (2004).
[3] T. Bolton et al., Phys. Rev. Lett. **69**, 1328 (1992).
[4] J.-Z. Bai et al. (BES Collaboration), Phys. Lett. B **446**, 356 (1999).
[5] J.-E. Augustin et al. (DM2 Collaboration), Phys. Rev. D **42**, 10 (1990).
[6] M. Ablikim et al. (BESIII Collaboration), Phys. Rev. Lett. **107**, 182001 (2011).
[7] G.S. Adams et al. (E852 Collaboration), Phys. Lett. B **516**, 264 (2001).
[8] M.G. Rath et al., Phys. Rev. D **40**, 693 (1989).
[9] F. Nichitiuet al. (OBELIX Collaboration), Phys. Lett. B **545**, 261 (2002).
[10] Z. Bai et al. (MARKIII Collaboration), Phys. Rev. Lett. **65**, 2507 (1990).
[11] J.-E. Augustin et al. (DM2 Collaboration), $\eta(1430)$ energy range, Phys. Rev. D **46**, 1951 (1992).
[12] S. X. Nakamura, H. Kamano, T. S. H. Lee and T. Sato, Phys. Rev. D **86** (2012), 114012
[13] M. Ablikim *et al.* [BESIII], JHEP **03** (2023), 121
[14] S. X. Nakamura, Q. Huang, J. J. Wu, H. P. Peng, Y. Zhang and Y. C. Zhu, Phys. Rev. D **107** (2023) no.9, L091505
[15] S. X. Nakamura, Q. Huang, J. J. Wu, H. P. Peng, Y. Zhang and Y. C. Zhu, [arXiv:2311.05391 [hep-ph]].
[16] M. Bando, T. Kugo, and K. Yamawaki, Phys. Rept. **164**, 217 (1988).